Research Article

http://dx.doi.org/10.21060/cis.2014.311

Nickel nanostructures synthesised by a simple thermal decomposition route

Kalpanadevi Kalimuthu, Sinduja Rangasamy, Manimekalai Rakkiyasamy*

Department of Chemistry, Kongunadu Arts and Science College, Coimbatore, Tamilnadu, India – 641 029.
*Email: manimekalaikasc@gmail.com

Received: October 26, 2014; accepted: December 12, 2014

Abstract: Ni nanoparticles (Ni-NPs) have been prepared from an inorganic precursor by thermal decomposition route. The prepared precursor $Ni(C_9H_7O_2)_2(N_2H_4)_2$ was characterised by hydrazine and metal analyses, infrared spectrum and thermo gravimetry. By the thermal treatment of the precursor under suitable conditions, Ni-NPs of average size around 23 nm were obtained. Nanostructured Ni particles thus synthesised were characterised by X-Ray Diffraction (XRD), High Resolution Transmission Electron Microscopic (HRTEM), Selected Area Electron Diffraction (SAED) and Scanning Electron Microscopic (SEM) techniques.

Keywords: *Ni-NPs; thermal treatment; XRD; HRTEM; SAED; SEM*

1. INTRODUCTION

With the increased demand for clean technologies and consciousness of the environmental issues, the use of nanotechnology has become imperative during the last few decades. Nanomaterials are receiving more importance in the swiftly budding field of nanotechnology because of their unique properties in contrast to the bulk equivalents. At nanometer size, the number of atoms at the surface becomes significantly more, which improves their properties to a greater extent. Due to their large surface area, nanomaterials possess numerous advantages when compared with the conventional materials in several applications. Interest and studies in nanometer-sized metal/metal-oxide particles with properties distinct from those of individual atoms and molecules or bulk matter have progressed rapidly over the recent years. The applications of nanomaterials in various fields, such as photoelectric, recording materials, catalysts, sensors, ceramic materials, paint pigments, cosmetics, pharmaceuticals, medical diagnostics, membranes and filters, batteries and fuel cells, electronics, magnetic and optical devices, flat panel displays, biomaterials, structured materials, and protective coatings, etc., due to their extraordinary structures and properties have been reported [1-4].

The applications of ferrimagnetic and ferromagnetic fine particles in many technologies, including the fields like magnetic separation, magnetic recording, drug delivery, hyperthermia treatments, MRI contrast agents [5, 6] have been studied extensively in the recent past. Ni-NPs, ferromagnetic in nature, are seeking considerable attention because of their valuable magnetic, catalytic and electronic properties which make them significantly applicable as catalysts, fuel cell electrodes, gas sensors, battery hybrids, magnetic sensors and memory devices to biomolecular separations [7-11].

Since the innovation of nano chemistry in past decades, a great many methods have been described by the research community to synthesise metal nanoparticles, such as sputtering [12], vacuum evaporation [13], electron beam deposition [14], thermal decomposition [15], pulsed laser ablation [16], Hydrothermal process [17,18] and so on. Many of these preparation methods are, however, very complicated and difficult to control. They may have the disadvantages of the need of expensive equipments and consumption of energy which limit their preference. Thermal decomposition method is more advantageous over the others due to its simple procedure, economically feasible process and the ease to produce nanomaterials of high purity, high crystallinity and large surface area.

Here, we have reported a detailed method of synthesis and characterisation of the inorganic precursor $Ni(C_9H_7)_2(N_2H_4)_2$ and the corresponding metal nanoparticles via a simple thermal decomposition route.

2. EXPERIMENTAL

2.1 Synthesis and characterisation of the precursor $Ni(C_9H_7O_2)_2(N_2H_4)_2$

This was obtained by adding 50 mL of an aqueous solution of hydrazine hydrate (0.5 mL, 0.001 mol) and cinnamic acid (0.74g 0.005 mol) to 50 mL of the aqueous solution of nickel nitrate hexahydrate (0.73 g, 0.002 mol). The instantly formed blue precipitate was set aside for an hour, then filtered, washed with water and alcohol followed by diethylether and dried in air.

The percentage of hydrazine present in the precursor was found out by titrating the sample solution against KIO_3 [19] and that

of nickel was estimated by the quantitative method illustrated in the Vogel's textbook [19]. The infrared spectrum of the solid precursor was recorded by the KBr disc technique using a Perkin Elmer 597/1650 spectrophotometer. Thermal analysis of the precursor sample was carried out in Shimadzu DT40, Stanton 781 and STA 1500 thermal analyzer, in air atmosphere from room temperature to 700 °C at the heating rate of 10 °C per minute using 5-10 mg of the sample.

2.2 Synthesis and characterization of Ni-NPs

Ni-NPs were obtained by the thermal decomposition of the precursor. In this method, the dried precursor sample was taken in a silica crucible and heated to red hot for about 45 minutes. The violent decomposition of $Ni(C_9H_7O_2)_2(N_2H_4)_2$ resulted in the formation of Ni-NPs, which are brought down to room temperature, ground well and stored in a desiccator.

The phase formation and purity of the as-synthesised nanoparticles were known from the XRD pattern recorded using an X-ray diffractometer (X'per PRO model) using CuKα radiation, at 40 keV in the 2θ range of 10–80˚. The particle size of the synthesised particles was determined by High Resolution Transmission Electron Microscopy (HRTEM) (Hitachi Model H-800 using an accelerating voltage of 200 kV). Morphological analysis was done with the help of a Scanning electron microscopy (SEM) (HITACHI Model S-3000H).

3. RESULTS AND DISCUSSION

3.1. Chemical formula determination of the precursor

A tentative chemical formula $Ni(C_9H_7O_2)_2(N_2H_4)_2$ has been fixed to the precursor, on the basis of the found values of hydrazine (15.00) and nickel (14.10) percentage which are found to best fit respectively with the calculated values (15.36) and (14.08) for hydrazine and nickel percentage.

3.2 IR spectral analysis of the precursor

In the IR spectrum of $Ni(C_9H_7O_2)_2(N_2H_4)_2$, a sharp band was noticed at 972 cm^{-1}, which corresponds to the N-N stretching frequency, explicitly proving that the hydrazine moieties are coordinated with the metal in a bidentate bridging fashion [20,21]. The carboxylate ion asymmetric and symmetric stretching frequencies were observed at 1612 and 1384 cm^{-1}, respectively with the Δυ value of 288 cm^{-1}, indicating the monodentate liganding of –COOH groups. An intense band at 3305 cm^{-1} showed the N-H stretching in the prepared precursor.

3.3 Thermal analysis of the precursor

Figure 1 shows the TG-DTA curves of the precursor. The weight loss occurs in two steps, the initial one being the exothermic dehydrazination of the precursor between 158-256 °C, which results in the formation of an unstable metal carboxylate intermediate. The final step which takes place from 251 to 470° C is ascribed to the decarboxylation of the dehydrazinated precursor, giving Ni metal as the final residue.

Characterization of Ni-NPs

3.4 XRD analysis

Figure 2 depicts the X-ray diffraction pattern of Ni-NPs. The three intense peaks in the whole spectrum of 2θ values range from 44˚ to 77˚. The strong diffraction peaks at 2θ values of 44.82˚, 52.18˚ and 76.70˚ correspond to the (1 1 1), (2 0 0) and (2 2 0) planes of a cubic pattern of Ni. All the peaks in the pattern are found to agree with the standard reference data of Ni [JCPDS card no. 03-1051]. From Debye-Scherrer equation, $D = K\lambda/\beta\cos\theta$, where, θ = Bragg diffraction angle, K = Blank's constant, λ = source wavelength (1.54) and β = the width of the XRD peak at half maximum height, the crystallite size is estimated to be around 23 nm. No other impurity peaks are present in the diffractogram, confirming the phase purity of the product.

3.5 HRTEM analysis

Figure 3 (a & b) pictures the HRTEM micrographs of the as-prepared Ni powders. The average particle size examined from

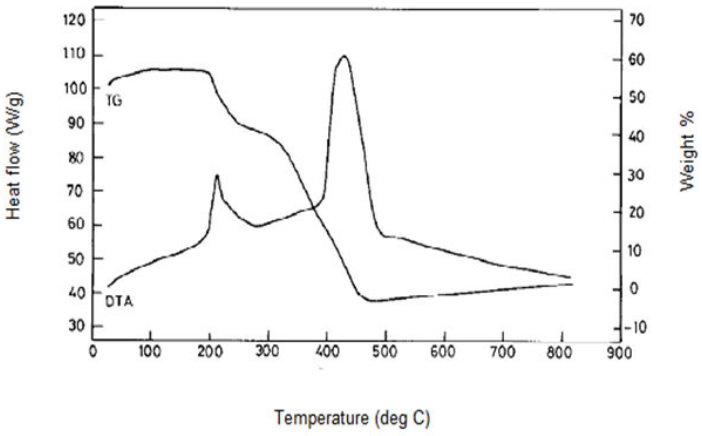

Figure 1: TG-DTA curve of $Ni(cin)_2(N_2H_4)_2$

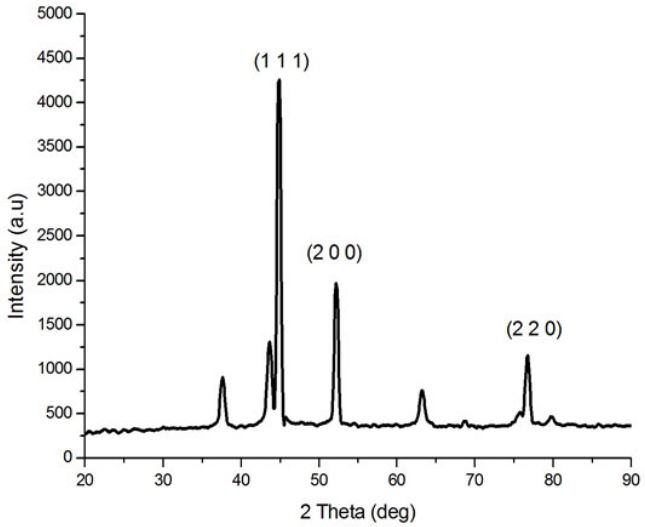

Figure 2: XRD pattern of Ni-NPs

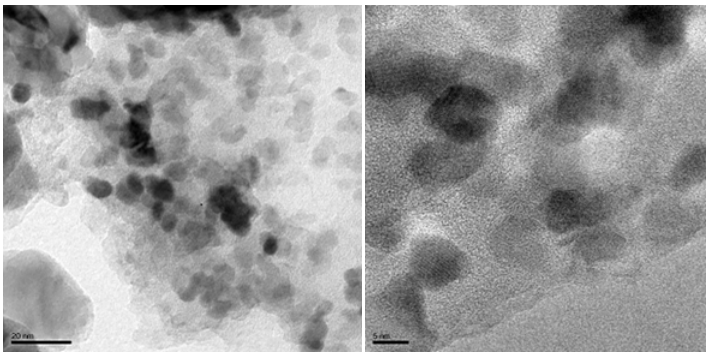

Figure 3: (a & b) – HRTEM micrograph of Ni-NPs

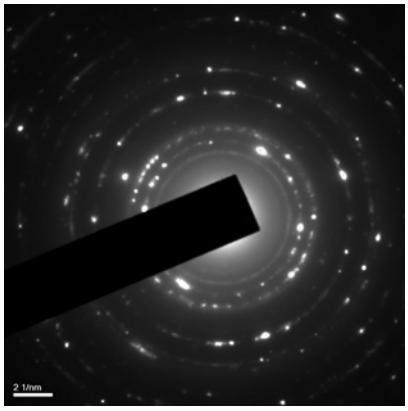

Figure 4: SAED pattern of Ni-NPs

the HRTEM images is about 23-25 nm, which agrees well with that estimated from the XRD. The selected area electron diffraction (SAED) pattern is shown in Figure 4 which indicates bright rings, revealing the polycrystalline nature of the sample.

3.6 SEM analysis

The scanning electron micrographs of the as-synthesised Ni-NPs are shown in Figures 5 (a & b). The SEM picture clearly shows nano-sized homogenous grains with the presence of a sizable number of agglomerated particles. The grains appear to stick each other and agglomerate in different masses throughout the micrograph. EDX spectrum of Ni-NPs Figure 6, provides the actual chemical composition of the sample. The EDX analysis suggests that Ni is the main constituent of the as-prepared nanoparticles.

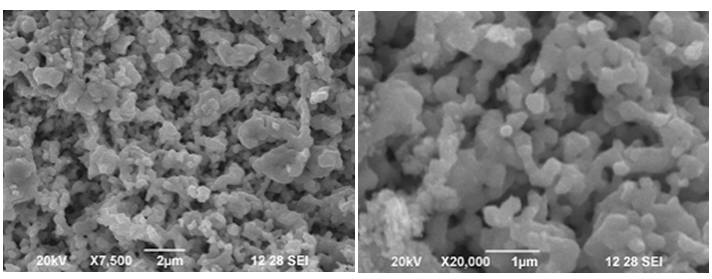

Figure 5 (a & b): SEM micrograph of Ni-NPs

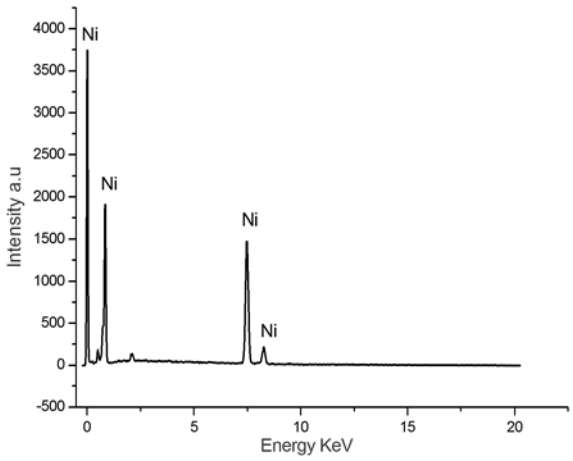

Figure 6: EDX spectrum of Ni-NPs

CONCLUSIONS

Nickel nanoparticles (Ni-NPs) were successfully synthesised by an effective thermal decomposition method. The inorganic precursor, $Ni(C_9H_7O_2)_2(N_2H_4)_2$ prepared was characterised by hydrazine and metal percentage analysis, IR spectral study and thermal analysis. Ni-NPs formed were characterized by XRD, HRTEM, SAED and SEM techniques. The average size of Ni-NPs is found to be 23 nm, as determined from XRD and HRTEM. Thus this method forms an easy, a simple and a commercially viable route to synthesize Ni-NPs.

REFERENCES

[1]. Kim, Y.S. and Kim, Y.H. *J. Mag. Mag. Mater*, **2003**, 267, 105.

[2]. Shi, J.J. ; Zhu, Y.F.; Zhang, X.R.; Willy, R.G.B. and Ana, R.G.C. *TrAC Trends Anal. Chem.*, **2004**, 23, 351.

[3]. Goswami, D.Y.; Vijayaraghavan, S.; Lu, S. and Tamm, G. *Sol. Energy*, **2004**, 76, 33.

[4]. Conte, M.; Prosini, P.P. and Passerini, S. *Mater. Sci. Eng., B* , **2004**, 108, 2.

[5]. Pankhurst, Q.A.; Connolly, J.; Jones, S.K. and Dobson, J. *J. Phys. D: Appl. Phys.* , **2003**, 36, R167.

[6]. Chen, D.X.; Pascu, O.; Roig, A. and Sanchez, A. *J. Mag. Mag. Mater*, **2010**, 322, 3834.

[7]. Del Bianco, L.; Boscherini, F.; Fiorini, A.L.; Tamisari, M.; Spizzo, F.; Vittori Antisari, M. and Piscopiello, E. *Phys. Rev. B*, **2008**, 77, 094408.

[8]. Nelson, P.A.; Elliott, J.M.; Attard, G.S. and Owen, J.R. *Chem. Mater.*, **2002**, 14, 524.

[9]. Del Bianco, L.; Boscherini, F.; Tamisari, M.; Spizzo, F.; Vittori Antisari, M. and Piscopiello, E. *J. Phys. D: Appl. Phys.*, **2003**, 41, 134008.

[10]. Huntz, A.M.; Andrieux, M. and Molins, R. *Mater. Sci. Eng., B*, **2006**, 415, 21.

[11]. Sakiyama, K.; Koga, K.; Seto, T.; Hirasawa, M. and Orii,

T. *J. Phys. Chem. B* , **2004**, 108, 523.

[12]. Ahn, K.S.; Nah, Y.C. and Sung, Y.E. *Appl. Surf. Sci.*, **2002**, 199, 259.

[13]. Porqueras, I. and Bertran, E. *Thin Solid Films*, **2001**, 41, 398.

[14]. Wu, Y.G.; Wu, G.M.; Ni, X.Y. and Wu, X. *Sol. Energy Mater. Sol. Cells* , **2000**, 63, 21.

[15]. Kalpanadevi, K.; Sinduja, C.R. and Manimekalai, R. *Mater Sci-Poland*, **2014**, 32, 34.

[16]. Wang, Y. and Qin, Q.-Z. *J. Electrochem. Soc.*, **2002**, 149, A873.

[17]. Liu, X.M.; Zhang, X.G. and Fu, S.Y. *Mater. Res. Bull.*, **2006**, 41, 620.

[18]. Liang, Z.H.; Zhu, Y.J. and Hu, X.L. *J. Phys. Chem. B*, **2004**, 108, 3488.

[19]. Jefferey, G.H.; Bassett, J.; Mendham, J. and Denney, R.C. Vogel's Textbook of Quantitative Chemical Analysis, Longman, UK, 5th Ed., **1989**.

[20]. Kalpanadevi, K.; Sinduja, C.R. and Manimekalai, R. *Acta Chim. Slov.*, **2013**, 60, 896.

[21] Braibanti, A.; Dallavalle, F.; Pellinghelli, M.A.; Leporati, E. *Inorg. Chem.* **1968**, 7, 1430–1433.